IEEE Access
Multidisciplinary | Rapid Review | Open Access Journal

Received January 12, 2021, accepted January 25, 2021, date of publication February 2, 2021, date of current version March 24, 2021.

Digital Object Identifier 10.1109/ACCESS.2021.3056388

Optimal Collaborative Expansion Planning of Integrated Cooling and Power System for Low-Latitude Distribution Networks

BO YANG[1], JUN TANG[1], ZHAO LUO[2], CHEN YANG[1], XIAOFENG DONG[1], JIALU GENG[2], YUNRUI JIA[2], AND HONGZHI LIU[2]

[1]State Grid Suzhou Power Supply Company, Suzhou 215004, China
[2]Faculty of Electric Power Engineering, Kunming University of Science and Technology, Kunming 650500, China

Corresponding author: Zhao Luo (waiting.1986@live.com)

This work was supported in part by the National Natural Science Foundation of China under Grant 51907084, in part by the AND Comprehensive Demonstration Project of Smart Grid Application Demonstration Area in Suzhou Industrial Park, in part by the Yunnan Provincial Talents Training Program under Grant KKSY201704027, and in part by the Scientific Research Foundation of the Yunnan Provincial Department of Education under Grant 2018JS032.

ABSTRACT In low latitudes, ice storage air conditioners (ISACs) have been widely used to cool while locally responding to the distribution network demand. However, due to the lack of the direct cold energy exchange between ISACs, the cooling load could only be shifted on the time scale instead of the space scale, resulting in an unsatisfactory regulation result. To address the above problem, this article proposes a novel collaborative expansion planning scheme for integrated cooling and power system. Firstly, to increase the regulation flexibility, a novel cold energy supply system is designed, where ice making stations and trucks are used to produce and deliver ices to multiple terminal ISACs. On this basis, taking the capacity of the wind turbines (WTs), large ice makers (LIMs), and trucks as configuration decisions, an optimal expansion planning model is established considering wind generation uncertainties. This model is converted into a classic mixed-integer second-order cone programming (MISOCP) problem using linear techniques, and efficiently solved by the Benders decomposition method. Finally, Shapley value method in economics is used to fairly distribute the revenues between the grid operator (GO) and ISAC owners. Simulation studies on IEEE 14-node distribution network indicate the proposed expansion model is effective and beneficial.

INDEX TERMS Low-latitude distribution network, ice storage air conditioners, expansion planning, integrated cooling and power system, Shapley value method, Benders decomposition method.

I. INTRODUCTION

With the awakening of energy crisis and environmental awareness, more and more renewable generation is connected to the distribution network [1]. It is found that the multi-energy systems which integrate multiple energy carriers and provide various energy services can further develop complementary advantages (e.g. efficiency improvement, cost savings, and so on) while accommodating renewable energy resources [2]. As an important form of the multi-energy systems, the integrated cooling and power system is believed to be more and more popular in low latitude region [3]. Therefore, it is worth studying the expansion planning of the low-latitude distribution network on integrated cooling and power system.

More recently, many researches have focused on the coordinated planning of the integrated electricity, heat and cooling multi-energy systems, including the system structure optimization [4]–[6], location, type, and capacity configuration of the common units [7]–[13], energy storage characteristic development [14]–[17], and uncertainty analysis [18]–[20]. For example, in [4], a generic structure planning and operation optimization scheme is proposed to obtain both the optimal structure configuration and energy management strategies of combined heating and power. In [5], a graph-theory-based optimal configuration planning framework for a community level integrated electricity-heat system is presented to determine the selection and connection of energy converters and devices. In [6], a two-stage model

The associate editor coordinating the review of this manuscript and approving it for publication was Siqi Bu.

for integrated heat and electricity system is established to optimize the connection relationships between the invested system components in each two adjacent layers and system component types for each layer. Additionally, an optimal planning model for a coupled combined cooling heating and power system is proposed in [7] to optimize the location and capacity of units. A comprehensive model for integrated heat and electricity system is used in [8] to find the best size and operation for elements of these systems according to historical analysis of utility demand. A new composite indicator for optimum sizing and operational strategy of combined heat and power plant is introduced in [9] to give a more comprehensive assessment of the performances. An optimal plant configuration approach for a specific commercial building is presented in [10], [11] to select the sizes and the number of cogeneration systems and the auxiliary equipment based on the annual demands of electricity, heating and cooling. A two-stage planning and design method for the integrated heat-electricity systems is proposed in [12] to obtain the optimal type and capacity of the equipment using the system parameters and load data. In [13], combined heat and power plant is optimally planned (placed and sized) at the network by considering the operation costs, power loss, network reliability, and voltage penalty. Moreover, a planning problem of the multi-energy systems considering the thermal storage capacity of the heating network and heat load is formulated in [14]. A mathematical model is developed in [15] to calculate the optimal capacities of the combined heat and power system and a storage tank and a back-up boiler. A thermal inertia aggregation model is established in [16], [17] for the planning and operation of integrated electricity-heat-gas systems considering the heat storage dynamic characteristics of district heating network and buildings. In addition, a combination of robust and stochastic optimization approaches is used in [18] for integrated electricity-heat-hydrogen system planning to address the generation-load uncertainties. A data-driven two-stage stochastic programming model is discussed in [19] for energy hub capacity planning. Considering the uncertainties of the heat load, ambient temperature and heat dissipation coefficients of heating pipelines, a two-stage robust integrated electricity and heating system scheduling strategy is studied in [20]. However, focusing on the integrated heating, (cooling) and power system planning, the existing literature rarely discuss the low latitude regions with strong cooling demands almost all year round. Unlike heating systems designed to supply the thermal loads of several or more kilometers, cooling system planning is generally limited to the community or building level due to economic factors and operation efficiency. Therefore, we cannot learn much from the existing works. Additionally, DC power flow model is widely used in the above literature to depict the electricity supply, which may result in planning scheme error, especially for distribution networks with serious power losses.

As a further study, the cooling and electricity combined scheduling of the distribution network have also received considerable attention recently. For example, [21], [22] establish a hierarchical control framework for distribution networks to management the refrigeration power of air conditioners. [23], [24] propose a planning scheme for ultra-deep mine cooling systems using chilled water and ice. References [25] and [26] discuss a planning and operation approach for data centers and telecommunications systems to achieve a multi-time scale cooling and electricity management. Reference [27] designs a cooling energy storage system in smart building based on phase change material, together with its corresponding cooling-electric combined two-stage dispatching strategy. Reference [28] develops an integrated cooling and power system based on cogeneration of a concentrating solar power plant and buildings with phase change materials. References [29] and [30] study the ice-storage air conditioners (ISACs) to carry out cutting peak and filling valley. Although the advantages of combined supply of cooling and electricity have been initially demonstrated, the energy-saving opportunities have not been fully exploited due to the disadvantages of not being able to exchange energy directly between cooling systems. In addition, considering that multiple cooling systems as well as the power system belong to different stakeholders, how to distribute the collaborative benefits is worth studying.

With the above observations, it can be speculated that more energy interaction among cooling systems and stronger coupling between cooling and power system can significantly increase the operation economy of low-latitude distribution networks. Motivated by the existing research gaps, a novel integrated cooling and power system expansion planning scheme for low-latitude distribution networks is proposed in this article. Firstly, without loss of generality, it is assumed that multiple ISACs have been used for refrigeration, and no renewable energy has been connected to the grid. To increase the collaborative optimization opportunities of distribution networks, not only wind turbines (WTs), but also a large ice maker (LIM) would be installed, where the ices produced would be delivered to the tanks of multiple ISACs to support cooling loads. Taking the uncertainties of wind generation into account, the expansion planning model of the novel integrated cooling and power system is established. On this basis, this model is converted as a classic mixed-integer second-order cone programming (MISOCP) problem, and solved by Benders decomposition method. Finally, simulation studies are conducted on IEEE 14-node distribution network. According to the optimization results, Shapley value method in economics is used to distribute expansion planning revenues fairly between the ISAC owners and grid operator (GO). The main contributions of this article are summarized as follows:

1) A novel integrated cooling and power collaborative expansion planning framework for low-latitude distribution networks is proposed. To promote the cooperation between ISAC owners and GO, Shapely value method in economics is used to distribute the planning revenues reasonably.

2) An integrated cooling and power system expansion planning model integrating robust method is established. Linear techniques and Benders decomposition method are used to solve this model efficiently.

3) Using realistic wind generation and load, the effectiveness and benefits of the proposed strategy is verified.

The rest of this article is organized as follows: Section II presents the framework of expansion planning of integrated cooling and power system. Section III introduces the novel expansion planning model. Solution algorithm is depicted in Section IV. Results and discussion are conducted in Section V. Finally, the conclusions are drawn in Section VI.

II. FRAMEWORK OF EXPANSION PLANNING OF INTEGRATED COOLING AND POWER SYSTEM FOR LOW-LATITUDE DISTRIBUTION NETWORKS

A. COLLABORATIVE EXPANSION PLANNING OF COOLING AND POWER SYSTEM

Figure 1 depicts a diagram of the ISAC. As observed from the figure, the ISAC includes a refrigeration pump, an ice maker, an ice melting unit, and an ice storage tank. Assume that the arrow represents the direction of the cold flow. The ISAC could store or melt ice while satisfying the cold demand of communities or buildings. By regulating the grid-connected power, ISACs are able to carry out demand response according to the time of use tariff price. However, due to the lack of the direct cold energy exchange between cooling systems, the cooling load could not be shifted on the space scale. Therefore, the effect of peak cutting and valley filling may be limited.

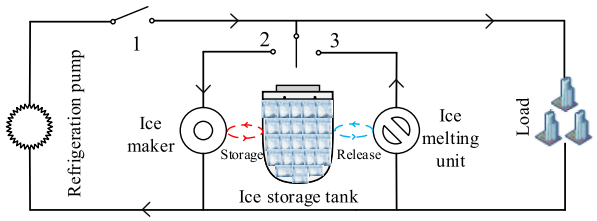

FIGURE 1. Diagram of ice storage air conditioners.

To operate the low-latitude distribution network better, this article proposes a novel collaborative expansion planning framework for integrated cooling and power system, as depicted in Figure 2. To reduce the energy demand of the local electric loads, WTs are installed to generate electricity. Meanwhile, in a light load area, a LIM is configured to produce ices. The ices produced are transported by trucks and then dropped into ice storage tanks of ISACs. By this method, not only the electricity, but also cooling energy could be directly exchanged. Therefore, the novel integrated cooling and power system would be better operated. Note that the it is common that ices are delivered based on trucks to cool residents and keep supermarket meat fresh [31]. Therefore, the proposed novel expansion planning strategy is technically feasible.

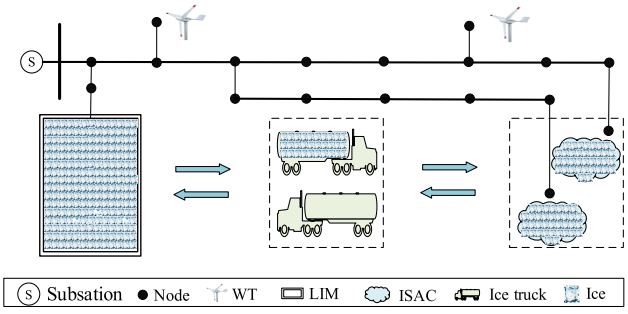

FIGURE 2. Collaborative expansion planning framework for integrated cooling and power system.

B. REVENUE DISTRIBUTION METHOD

Generally, the GO is responsible for distribution network expansion planning, while the community property owns ISACs. They belong to different stakeholders. Although the WTs and LIMs as well as trucks could be invested and operated by the grid operator, ISACs must participate in the integrated cooling and power system schedule. Therefore, the grid operator and community property shall be cooperated. To fairly distribute the revenues according to participator's contributions, Shapley value method in economics is used in this article [32]. More descriptions are given as follows:

Define that set $N = \{1,2, \cdots, n\}$ stands for n members involved in an economic activity, S means a subset of N, V(S) denotes the cooperative revenue. Their relationships are written in (1).

$$\begin{cases} V(\phi) = 0 \\ V(S_1 \cup S_2) \geq V(S_1) + V(S_2) \end{cases} \quad S_1 \cap S_2 = \phi \qquad (1)$$

Assume that $\Phi_i(\upsilon)$ represents the revenues of member i, $\Phi = (\Phi_1(\upsilon), \Phi_2(\upsilon), \cdots, \Phi_n(\upsilon))$ indicates the revenue distribution vector, as follows:

$$\Phi_i(\upsilon) = \sum_i w(|S|)(\upsilon(S) - \upsilon(S \backslash i)), \quad i = 1, 2, \ldots, n \qquad (2)$$

$$w(|S|) = (n - |S|)!(|S| - 1)!/n! \qquad (3)$$

where $|S|$ and n stand for the subset number and member number, respectively, and $\upsilon(S \backslash i)$ is the contribution of member i in S.

Without loss of generality, assume that the grid operator (i.e., GO) and two ISACs (i.e., ISAC1 and ISAC 2) are engaged in the integrated cooling and power system. In this case, there are seven possible economies, i.e., S = ({GO}, {ISAC1}, {ISAC2}, {GO, ISAC1}, {GO, ISAC2}, {ISAC1, ISAC2}, {GO, ISAC1, ISAC2}). The revenue space and distribution vector can be represented as $V = (\upsilon(\{GO\}), \upsilon(\{ISAC1\}), \upsilon(\{ISAC2\}), \upsilon(\{GO, ISAC1\}), \upsilon(\{GO, ISAC2\}), \upsilon(\{ISAC1, ISAC2\}, \upsilon(\{GO, ISAC1,ISAC2\}))$, and $\Phi = (\Phi_1(\upsilon), \Phi_2(\upsilon), \Phi_3(\upsilon), \Phi_4(\upsilon), \Phi_5(\upsilon), \Phi_6(\upsilon), \Phi_7(\upsilon))$, respectively.

III. EXPANSION PLANNING MODEL OF THE INTEGRATED COOLING AND POWER SYSTEM FOR LOW-LATITUDE DISTRIBUTION NETWORKS

A. OBJECTIVE

The expansion planning costs consist of investment costs and operation costs. The investment body includes WTs, LIMs and trucks, while the operation costs come from the truck, load shedding (LS), and external grid (EG), as follows:

$$C^{Total} = \left(C_I^{WT} + C_I^{LIM} + C_I^{Truck}\right) + \left(C_O^{Truck} + C_O^{EG} + C_O^{LS}\right) \tag{4}$$

where C^{Total} indicates the total expansion planning cost, C_I^{WT}, C_I^{Truck}, and C_I^{LIM} represent the investment costs of the WTs, trucks and LIMs, respectively, C_O^{Truck}, C_O^{EG}, and C_O^{LS} denote the costs of the truck driving, purchasing electricity from the EG, and LS penalty, respectively.

The detailed explanations are presented as follows:

$$C_I^{WT} = \sum_i \left(P_i^{WT} p^{WT}\right) \times \frac{r\,(1+r)^{y^{WT}}}{\left((1+r)^{y^{WT}} - 1\right)} \tag{5}$$

$$C_I^{LIM} = \sum_i \left(P_i^{LIM} p^{LIM}\right) \times \frac{r\,(1+r)^{y^{LIM}}}{\left((1+r)^{y^{LIM}} - 1\right)} \tag{6}$$

$$C_I^{Truck} = C^{Truck} \times \frac{r\,(1+r)^{y^{Truck}}}{\left((1+r)^{y^{Truck}} - 1\right)} \tag{7}$$

$$C_O^{Truck} = \sum_{s=1}^{S}\sum_{t=1}^{T}\left(\sum_{i\neq j} I_{s,t}^{ij} p^{fuel} + C^{Labor}\right) \tag{8}$$

$$C_O^{EG} = \sum_{s=1}^{S}\sum_{t=1}^{T}\left(p_t^{EG} P_{s,t}^{EG}\right) \tag{9}$$

$$C_O^{LS} = \sum_{s=1}^{S}\sum_{t=1}^{T}\left(p^{LS} P_{s,t}^{LS}\right) \tag{10}$$

where p^{WT}, P_i^{WT}, and y^{WT} mean the investment prices, configuration capacity, and service lives of WTs, respectively, r represents the interest rate, p^{LIM}, p_I^{LIM}, and y^{LIM} are the investment prices, configuration capacity, and service lives of LIMs, respectively, C^{Truck} and y^{Truck} indicate the sale price and service lives of trucks, respectively, S and T express the scenario number and dispatching cycle, respectively, S denotes the hourly truck fuel cost, binary variable T means the truck driving flag from station i to station j at time t in scenario s, C^{Labor} is the driver labor cost, $P_{s,t}^{EG}$ and P_t^{EG} represent the EG power and price, respectively, $P_{s,t}^{LG}$ and P^{LS} stand for the LS amount, and penalty price, respectively.

To ensure the economy of the expansion planning scheme, the impact of the uncertainties must be considered. With regard to the proposed integrated cooling and power system, compared with the load power, the prediction error of wind generation is larger. For simplicity, only wind generation uncertainty is analyzed. Define $P_{s,i,t}^{WT}$ denotes the grid-connected wind power, it can be expressed as follows:

$$P_{s,i,t}^{WT} \le \rho_{s,i,t}^{WT} \times P_i^{WT} \tag{11}$$

where $P_{s,i,t}^{WT}$ denotes the wind generation per unit of installed capacity, respectively, P_i^{WT} represent the installed capacity of WTs at node i, respectively.

Considering the prediction errors, we build a robust model to construct an uncertain set of $P_{s,i,t}^{WT}$, as follows:

$$\begin{cases} \rho_{s,i,t}^{WT} \le \rho_{s,i,t}^{WT*}\left(1 + \Gamma\varepsilon^{WT}\right) : & \xi_{s,i,t}^{WT,1} \\ \rho_{s,i,t}^{WT} \ge \rho_{s,i,t}^{WT*}\left(1 - \Gamma\varepsilon^{WT}\right) : & \xi_{s,i,t}^{WT,2} \end{cases} \tag{12}$$

where $\rho_{s,i,t}^{WT*}$ represents the prediction power, ε^{WT} express the maximum deviation of WT output, Γ is used to control the conservative of the robustness of the problem.

According to duality theory, we can use feasible dual variables $\xi_{s,i,t}^{WT,1}$, and $\xi_{s,i,t}^{WT,2}$ to deal with the robust problem [33]. The objective function of expansion planning model considering uncertainties is represented as follows:

$$\min \quad C^{Total} \tag{13}$$

$$s.t. \begin{cases} \xi_{s,i,t}^{WT,1}\rho_{s,i,t}^{WT*}\left(1+\Gamma\varepsilon^{WT}\right) \times P_i^{WT} \\ \quad -\xi_{s,i,t}^{WT,2}\rho_{s,i,t}^{WT*}\left(1-\Gamma\varepsilon^{WT}\right) \times P_i^{WT} \le -P_{s,i,t}^{WT} \\ \xi_{s,i,t}^{WT,1} - \xi_{s,i,t}^{WT,2} \ge -1 \\ \xi_{s,i,t}^{WT,1}, \xi_{s,i,t}^{WT,2} \ge 0 \end{cases} \tag{14}$$

B. CONSTRAINTS

1) TRUCK TRANSIT CONSTRAINTS

Trucks are used to transport ices between LIMs and ISACs. Define H_m^{Ice} and $H_{s,i,t}^{Ice}$ represent the rated and real-time ice throughput capacity of the truck, respectively, E_m^{Truck} and $E_{s,t}^{Truck}$ denote the rated and real-time ice loading capacity of the truck, respectively, ξ^{air} represents the ice retention rate considering the cold leakage. Note that $I_{s,ii,t}$ denotes that the EV is located at station i. The location and loading constraints are presented as follows:

$$\sum_{ij} I_{s,ij,t} = 1 \tag{15}$$

$$\sum_{j} I_{s,ij,t+1} \ge I_{s,ii,t} \tag{16}$$

$$\sum_{k\neq i} I_{s,jk,t+1} \ge I_{s,ij,t} \tag{17}$$

$$\sum_{i} I_{s,ij,1} = I_{s,ii,0} \tag{18}$$

$$I_{s,ii,T} = I_{s,ii,0} \tag{19}$$

$$-H_m^{Ice} I_{s,ii,t} \le H_{s,i,t}^{Ice} \le H_m^{Ice} I_{s,ii,t} \tag{20}$$

$$E_{s,t}^{Truck} = E_{s,t-1}^{Truck}\xi^{air} + \sum H_{s,i,t}^{Ice} \tag{21}$$

$$0 \le E_{s,t}^{Truck} \le E_m^{Truck} \tag{22}$$

$$E_{s,t}^{Truck} = E_{s,0}^{Truck} \tag{23}$$

where (15) constrains the uniqueness of the location of the truck in time and space, (16)-(18) express the continuity of the

truck trip sequence, (19) requires the truck to return to initial location, (20) indicates the constraint of the ice throughput, (21)-(23) stand for the ice load limits of the truck.

2) OPERATIONAL CONSTRAINTS OF LARGE ICE MAKERS

LIMs are established to produce ices. Define $P_{s,i,t}^{LIM}$ and $P_{m,i}^{LIM}$ denote the real-time and rated ice making power, respectively, η^{ice} is the ice making efficiency, $E_{s,i,t}^{LIM}$ represents the amount of ice storage. The operational constraints are presented as follows:

$$0 \le P_{s,i,t}^{LIM} \le P_{m,i}^{LIM} \tag{24}$$

$$E_{s,i,t}^{LIM} = E_{s,i,t-1}^{LIM}\xi^{air} + P_{s,i,t}^{LIM}\eta^{ice} - H_{s,i,t}^{Ice} \tag{25}$$

$$0 \le E_{s,i,t}^{LIM} \le E_{m,i}^{LIM} \tag{26}$$

$$E_{s,i,T}^{LIM} = E_{s,i,0}^{LIM} \tag{27}$$

where (24) denotes the ice making power limit, (25)-(27) express the ice storage constraints.

3) OPERATIONAL CONSTRAINTS OF ICE STORAGE AIR CONDITIONERS

Define $P_{s,i,t}^{AC,chiller}$ and $P_{m,i}^{AC,chiller}$ as the actual and rated refrigeration power of ISACs, respectively, $P_{s,i,t}^{AC,ice}$ and $P_{m,i}^{AC,melt}$ stand for the real-time and rated ice making power, respectively, $P_{s,i,t}^{AC,melt}$ and denote the real-time and rated ice melting power, respectively, $\eta^{chiller}$, η^{ice} and η^{melt} represent the refrigeration, ice-making and ice-melting efficiency, $H_{s,i,t}^{l}$ is the cooling load, $E_{s,i,t}^{AC,ice}$ and $E_{m,i}^{AC,ice}$ express the real-time and rated ice storage capacity, respectively. The relationship between variables are given as follows:

$$0 \le P_{s,i,t}^{AC,chiller} \le P_{m,i}^{AC,chiller} \tag{28}$$

$$0 \le P_{s,i,t}^{AC,ice} \le P_{m,i}^{AC,ice} \tag{29}$$

$$0 \le P_{s,i,t}^{AC,melt} \le P_{m,i}^{AC,melt} \tag{30}$$

$$P_{s,i,t}^{AC,melt}\eta^{chiller} + P_{m,i}^{AC,melt}\eta^{melt} = H_{s,i,t}^{l} \tag{31}$$

$$E_{s,i,t}^{AC,ice} = E_{s,i,t-1}^{AC,ice}\xi^{air} + H_{s,i,t}^{Ice} + P_{s,i,t}^{AC,ice}\eta^{ice} - P_{s,i,t}^{AC,melt}\eta^{melt} \tag{32}$$

$$0 \le E_{s,i,t}^{AC,ice} \le E_{m,i}^{AC,ice} \tag{33}$$

$$E_{s,i,T}^{AC,ice} = E_{s,i,0}^{AC,ice} \tag{34}$$

where (28)-(30) express the constraints of refrigeration, ice-making, and ice-melt power, respectively, (31) denotes the cooling power balance limit, (32)-(34) represent the ice storage limits.

4) POWER FLOW CONSTRAINTS

Define $P_{s,i,t}$ and $Q_{s,i,t}^{l}$ represent the active and reactive power of the load at node i, respectively, $P_{s,i,t}$ and $Q_{s,i,t}$ denote the node injection active and reactive power, respectively, r_{ij} and x_{ij} stand for the resistance and reactance of branch ij, respectively, $\ell_{s,ij,t}$ and $\bar{\ell}_{ij}$ mean the square of the real-time and rated currents of branch ij, respectively, $P_{s,ji,t}$ and $Q_{s,ji,t}$ indicate the active power and reactive power of branch ij, respectively, $v_{s,i,t}$, $\bar{v_i}$, and $\underline{v_i}$ denote the real-time, maximum, and minimum voltages of node i, respectively. The power flow constraints are given as follows:

$$P_{s,i,t} = P_{s,i,t}^{l} - P_{s,i,t}^{WT} + P_{s,i,t}^{LIM} + P_{s,i,t}^{AC,ice} + P_{s,i,t}^{AC,melt} + P_{s,i,t}^{AC,chiller} \tag{35}$$

$$Q_{s,i,t} = Q_{s,i,t}^{l} - Q_{s,i,t}^{WT} + Q_{s,i,t}^{LIM} + Q_{s,i,t}^{AC,ice} + Q_{s,i,t}^{AC,melt} + Q_{s,i,t}^{AC,chiller} \tag{36}$$

$$P_{s,i,t} = -\sum_{j} P_{s,ij,t} \tag{37}$$

$$Q_{s,i,t} = -\sum_{j} Q_{s,ij,t} \tag{38}$$

$$P_{s,ji,t} = P_{s,ij,t} - r_{ij}\ell_{s,ij,t} \tag{39}$$

$$Q_{s,ji,t} = Q_{s,ij,t} - x_{ij}\ell_{s,ij,t} \tag{40}$$

$$\ell_{s,ij,t} = \left(P_{s,ij,t}^{2} + Q_{s,ij,t}^{2}\right) \Big/ v_{s,i,t} \tag{41}$$

$$\ell_{s,ij,t} \le \overline{\ell_{ij}} \tag{42}$$

$$\underline{v_i} \le v_{s,i,t} \le \overline{v_i} \tag{43}$$

where (35)–(36) indicate the node injection power constraints, (37)-(38) express the relationships between the node injection power and branch power, (39)-(40) represent the relationships between the injected power and outflow power of the branch ij, (41)-(43) mean the nodal voltage and branch current limits.

IV. SOLUTION ALGORITHM

A. LINEARIZATION STAGE

The optimization model includes several nonlinear constraints such as $\xi_{s,i,t}^{WT,1} \times P_i^{WT}$ and $\xi_{s,i,t}^{WT,2} \times P_i^{WT}$ of (14), which makes it difficult to be solved. To address this problem, linear techniques are used as follows:

First, assume P^{WT} denotes the rated capacity of a WT, N is the maximum possible installation number of WTs, binary variable $u_{n,i}^{WT}$ (n = 1,2,...,N) represents the installation mark of nth WT, $P_{n,s,i,t}^{WT,1}$ and $P_{n,s,i,t}^{WT,2}$ expresses $u_{n,i}^{WT}\xi_{s,i,t}^{WT,1}$ and $u_{n,i}^{WT}\xi_{s,i,t}^{WT,2}$, respectively. The corresponding relationships are presented as follows:

$$P_i^{WT} = \sum_{n=1}^{N} u_{n,i}^{WT} P^{WT} \tag{44}$$

$$\begin{cases} 0 \le P_{n,s,i,t}^{WT,1} \le \xi_{s,i,t}^{WT,1} P^{WT} \\ \xi_{s,i,t}^{WT,1} P^{WT} - M + u_{n,i}^{WT} M \le P_{n,s,i,t}^{WT,1} \le u_{n,i}^{WT} M \end{cases} \tag{45}$$

$$\begin{cases} 0 \le P_{n,s,i,t}^{WT,2} \le \xi_{s,i,t}^{WT,2} P^{WT} \\ \xi_{s,i,t}^{WT,2} P^{WT} - M + u_{n,i}^{WT} M \le P_{n,s,i,t}^{WT,2} \le u_{n,i}^{WT} M \end{cases} \tag{46}$$

where M is a large positive number.

According to (44)-(46), (11) can be replaced as follows:

$$\begin{cases} \rho_{s,i,t}^{WT*}\left(1+\Gamma\varepsilon^{WT}\right) ds \sum_{n=1}^{N} P_{n,i,s,t}^{WT,1} \\ \quad -\rho_{s,i,t}^{WT*}\left(1-\Gamma\varepsilon^{WT}\right) ds \sum_{n=1}^{N} P_{n,i,s,t}^{WT,2} \le -P_{s,i,t}^{WT} \\ \xi_{s,i,t}^{WT,1}-\xi_{s,i,t}^{WT,2} \ge -1 \\ \xi_{s,i,t}^{WT,1}, \xi_{s,i,t}^{WT,2} \ge 0 \end{cases} \quad (47)$$

Additionally, in the distribution network, (41) can be relaxed to the inequality (48) according to [34], and then is equivalently treated as the second-order cone limit in (49).

$$\ell_{ij,t} v_{i,t} \ge P_{ij,i,t}^2 + Q_{ij,i,t}^2 \quad (48)$$

$$\left\| \begin{matrix} 2P_{ij,i,t} \\ 2Q_{ij,i,t} \\ \ell_{ij,t}-v_{i,t} \end{matrix} \right\|_2 \le \ell_{ij,t}+v_{i,t} \quad (49)$$

Through the above process, the optimization model is converted as a classic MISOCP problem.

B. BENDERS SOLUTION STAGE

Define $\boldsymbol{x}=\left[u_{n,i}^{WT}, P_i^{WT}, P_{m,i}^{LIM}, I_{s,i\,j,t}\right]$ and

$$\boldsymbol{y}=\left[P_{s,i,t}, P_{s,i,t}^{WT}, P_{s,i,t}^{LIM}, P_{s,i,t}^{AC,i\,ce}, P_{s,i,t}^{AC,melt}, P_{s,i,t}^{AC,chiller}\right.$$
$$Q_{s,i,t}, Q_{s,i,t}^{WT}, Q_{s,i,t}^{LM}, Q_{s,i,t}^{ACice}, Q_{s,i,t}^{AC,melt}, Q_{s,i,t}^{AC,\,\text{chiller}}, P_{s,i\,j,t},$$
$$Q_{s,i\,j,t}, \ell_{s,i\,j,t}, v_{s,i,t}, E_{s,i,t}^{AC,i\,ce}, E_{s,i,t}^{Ice}, E_{s,t}^{Truck}, H_{s,i,t}^{Ice}, \xi_{s,i,t}^{WT,1},$$
$$\left.\xi_{s,i,t}^{WT,2},\right]$$

, the MI-SOCP problem can be denoted as follows:

$$min\ \boldsymbol{\kappa}^T\boldsymbol{x}+\boldsymbol{c}^T\boldsymbol{y} \quad (50\text{-}1)$$
$$s.t\ A\boldsymbol{x} \le \boldsymbol{b} \quad (50\text{-}2)$$
$$B\boldsymbol{x}+\boldsymbol{D}\boldsymbol{y} \le \boldsymbol{d} \quad (50\text{-}3)$$
$$\boldsymbol{E}\boldsymbol{y} \le \boldsymbol{e} \quad (50\text{-}4)$$
$$\|\boldsymbol{F}\boldsymbol{y}\|_2 \le \boldsymbol{f}\boldsymbol{y} \quad (50\text{-}5)$$

where $\boldsymbol{\kappa}, \boldsymbol{c}, A, \boldsymbol{b}, B, \boldsymbol{D}, \boldsymbol{d}, \boldsymbol{E}, \boldsymbol{e}, \boldsymbol{F}$, and $\boldsymbol{f}$ are the coefficient.

To solve the MI-SOCP problem efficiently, Benders decomposition method is used in this article. The sub-problem SP1 can be denoted as follows:

$$\begin{aligned} &\min\ \boldsymbol{c}^T\boldsymbol{y} \\ &s.t\ \boldsymbol{D}\boldsymbol{y} \le \boldsymbol{d}-B\bar{\boldsymbol{x}} \\ &\quad \boldsymbol{E}\boldsymbol{y} \le \boldsymbol{e} \\ &\quad \|\boldsymbol{F}\boldsymbol{y}\|_2 \le \boldsymbol{f}\boldsymbol{y} \end{aligned} \quad (51)$$

where $\bar{x}$ can be obtained from the main problem.

On this basis, we can obtain sub-problem SP2 according to duality theory, as follows:

$$\begin{aligned} &\max\ \ [\boldsymbol{d}-B\bar{\boldsymbol{x}}]^T\boldsymbol{u}+\boldsymbol{e}\boldsymbol{v} \\ &s.t\ \boldsymbol{D}\boldsymbol{u} \le \boldsymbol{E}\boldsymbol{v}+\boldsymbol{F}\theta-\boldsymbol{f}\pi+\boldsymbol{c}=0 \\ &\quad \|\boldsymbol{\theta}\|_2 \le \boldsymbol{\pi} \end{aligned} \quad (52)$$

where $\boldsymbol{u}, \boldsymbol{v}, \boldsymbol{\theta}$, and $\boldsymbol{\pi}$ are dual variables.

By solving (52), the upper bound U_B of the optimization problem can be expressed as follows:

$$U_B = \boldsymbol{\kappa}^T\bar{\boldsymbol{x}}+[\boldsymbol{d}-B\bar{\boldsymbol{x}}]^T\boldsymbol{u}+\boldsymbol{e}\boldsymbol{v} \quad (53)$$

On the other hand, the main problem can be denoted as follows:

$$\begin{aligned} &\min\ \ \boldsymbol{z} \\ &s.t.\ \boldsymbol{z} \ge \boldsymbol{\kappa}^T\boldsymbol{x}+[\boldsymbol{d}-B\boldsymbol{x}]^T\bar{\boldsymbol{u}}+\boldsymbol{e}\bar{\boldsymbol{v}} \\ &\quad A\boldsymbol{x} \le \boldsymbol{b} \end{aligned} \quad (54)$$

where $\bar{\boldsymbol{u}}$ and $\bar{\boldsymbol{v}}$ are obtained from sub-problem.

Define L_B as the lower bound of the optimization problem:

$$L_B = \boldsymbol{z} \quad (55)$$

The bounds U_B and L_B are solved iteratively until the following termination conditions are satisfied:

$$U_B - L_B \le \varepsilon \quad (56)$$

where ε stands for errors.

The detailed solution steps are given as follows:

Step 1: Initialization. Input investment price, common load, cooling load, wind power, electricity price, unit operation parameter, distribution network, $\bar{\boldsymbol{u}}$, $\bar{\boldsymbol{v}}$, ε

and so on.

Step 2: Solve main problem (54) and then calculate L_B according to (55). The optimization result of $\boldsymbol{x}$ is written as $\bar{\boldsymbol{x}}$, and then transferred to the sub-problem.

Step 3: Solve sub-problem (52)-(53) and update U_B.

Step 4: Check stopping criteria. If (56) is satisfied, the iterative process is terminated. Otherwise, go to step 2.

Step 5: The optimal planning results are obtained.

The flow chart of Benders decomposition method is depicted in Figure 3.

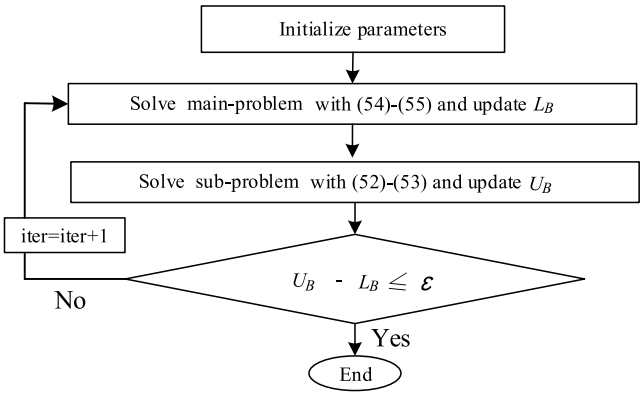

FIGURE 3. Flow chart of the Benders decomposition method.

V. RESULTS AND DISCUSSION

A. TEST SYSTEM

To verify the superiority of the proposed strategy, an IEEE-14 node distribution network depicted in Figure 4 is tested [35]. The reference voltage and capacity are 22 kV, and 100 MVA,

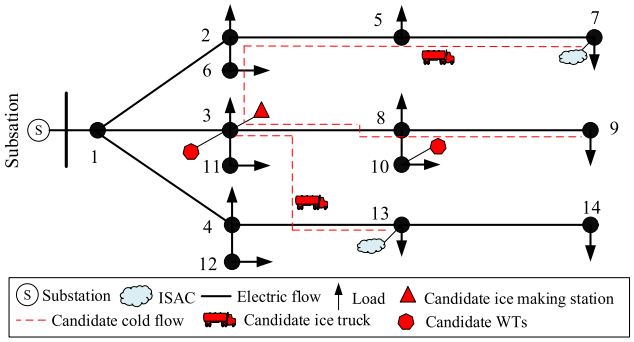

FIGURE 4. Diagram of the novel integrated cooling and power system.

TABLE 1. Distribution network parameters

Branch	R (p.u.)	X (p.u.)	Branch	R (p.u.)	X (p.u.)
1-2	0.30	0.4	8-9	0.32	0.44
1-3	0.44	0.44	8-10	0.44	0.44
1-4	0.44	0.44	3-11	0.44	0.44
2-5	0.36	0.72	4-12	0.36	0.48
2-6	0.32	0.44	4-13	0.16	0.44
5-7	0.16	0.16	13-14	0.16	0.16
3-8	0.32	0.44			

respectively. The nodal voltages are allowed to vary between 1.07 and 0.93. The distribution network parameters are shown in Table 1. Two ISACs are connected to the distribution network. Candidate WTs are allowed to install at nodes 3 and 10, while candidate ice making station is required to locate at node 3. The distances between the ice making station and ISACs are set to 20 km. A candidate truck is used to transport ices.

The EG electricity prices are 0.36 yuan at 0:00-7:00 and 23:00-24:00, 0.7 yuan at 7:00-10:00 and 13:00-18:00, 1.05 yuan at 10:00-13:00 and 18:00-23:00, respectively [36]. The annual power of common loads, cooling loads, and wind generation are collected from South China's low latitude regions. On this basis, they are clustered into three scenarios using the scenario reduction method [13]. Figure A1 in Appendix depicts the profiles of the electric load based on 100 MW, wind power based on 0.5-MW installing capacity, and cooling power based on 100 MW. The rated refrigeration power, ice making power, and melt power of ISACs are 7 MW, 20 MW, and 2 MW, respectively. The refrigeration, ice-making and ice-melt efficiencies are 4.2, 2.8, and 42.5, respectively [29]. The wind generation error and ice retention rate are 10%, and 98%, respectively.

The investment costs of WTs with a 30-year service life, LIMs with a 30-year life, and trucks with a 10-year life are 5100 yuan/kW, 1000 yuan/kW, and 400000 yuan respectively [37]. The driving speed and transportation cost of trucks are 20 km and 600 yuan per hour. According to China's market prices, the annual driver labor cost is set to 200000 yuan.

To verify the superiority of the proposed strategy, three cases are set to compare the operation results of the distribution network, as follows:

Case 1: Nothing would be configured in the distribution network.

Case 2: Only wind turbines would be installed in the distribution network.

Case 3: Not only the wind turbines, but also the ice making stations and trucks would be configured collaboratively.

Based on a 64-b Windows-based PC with i7 CPU @ 4.3 GHz, and 16 GB RAM, all numerical simulations are coded in MATLAB 2019b and solved using yalmip with Gurobi.

B. NUMERICAL SIMULATION RESULTS

Based on simulation parameters in subsection A, section IV, the expansion planning results of the integrated cooling and power system are obtained. The detailed explanations are presented as follows:

1) CASE 1

In this case, no equipment is added to the distribution network, where the external power grid and ISACs are the only power and cooling sources, respectively. Figure 5 shows the operation power and costs of integrated cooling and power system in typical scenarios. As observed from the figure, according to the time of use tariff price, the ISACs make every effort to consume more low-valley electricity and less high-peak power to satisfy the cooling demands. Even though the external grid can provide more power, due to the constraints of power flow and voltage level, 56.49 MWh, 58.69 MWh and 53.54 MWh electricity have to be cut off in three scenarios, respectively. It is indicated that the original distribution network needs to be transformed with regard to the reliability of power supply.

Table 2 illustrates the comprehensive operational cost of distribution network. As observed from the table, total expenses of integrated cooling and power system are 196666000 yuan, which includes the load shedding cost of 28026000 yuan, and purchasing electricity cost of 168640000 yuan. In this case, the daily operational cost constitutes the comprehensive cost of the distribution network.

TABLE 2. Costs of distribution network in three cases.

	Annual depreciation cost (yuan)		Annual operation cost (yuan)			Total cost (yuan)
	WT	LIM	Load shedding	Purchasing electricity	Truck and driver	
Case 1	0	0	28026000	168640000	0	196666000
Case 2	44240000	0	0	5551500	0	49791500
Case 3	30083000	2115200	0	3497000	970000	36665200

2) CASE 2

In this case, wind turbines are configured in the original distribution network, where both the wind generation and external grid could support the electric loads. Table 3 and Figure 6 depict the capacity configuration and operation results of integrated cooling and power system.

By installing 150-MW WTs, the power flow constraints of the distribution network can be satisfied more easily.

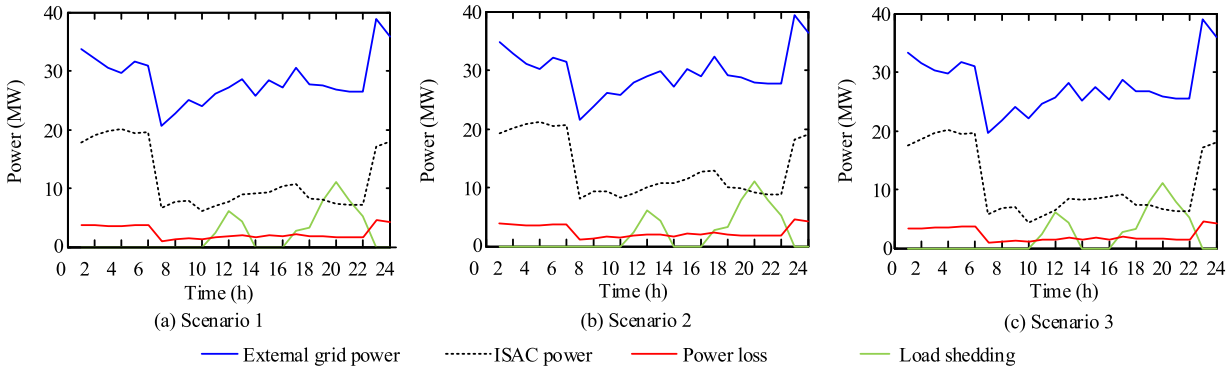

FIGURE 5. Operation power of integrated cooling and power system in case 1.

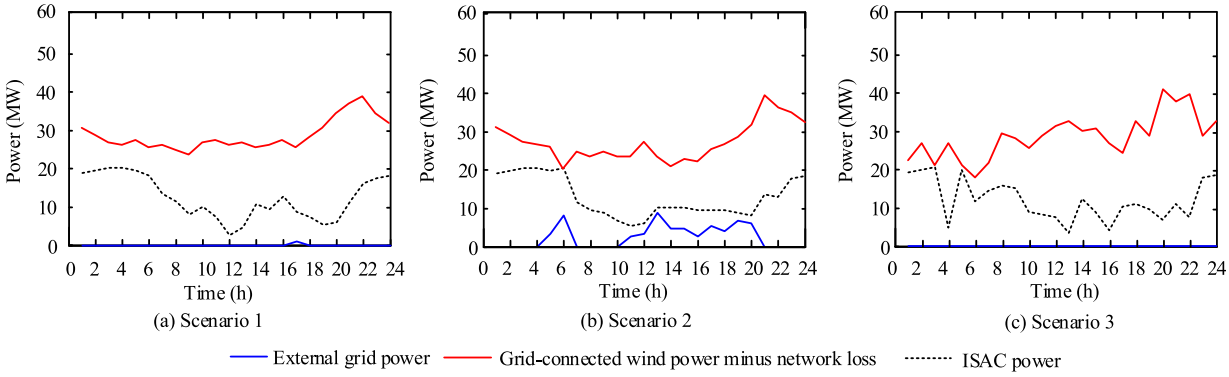

FIGURE 6. Operation power of integrated cooling and power system in case 2.

TABLE 3. Results of unit capacity configuration in three cases.

	WT at node 3 (MW)	WT at node 10 (MW)	LIM at node 3 (MW)
Case 1	0	0	0
Case 2	102	48	0
Case 3	96	6	37

Therefore, the load shedding does not occur. Additionally, benefiting from the wind generation, the purchasing electricity from the external grid are reduced significantly compared with that in case 1. However, the operating power of ISACs is basically unchanged with the same cooling system.

According to Table 2, the annual depreciation expense, annual operation cost, and comprehensive cost of the distribution network are 44240000 yuan, 5551500 yuan, 49791500 yuan, respectively. Compared with that in case 1, the total annual operation costs of integrated cooling and power system in case 2 are reduced by 146874500 yuan (74.7 %). The results demonstrate that the common expansion scheme can improve the economy of the distribution network.

3) CASE 3

In this case, both the WTs and LIMs as well as truck are configured in the distribution network, where multiple sources could supply the electric and cooling loads.

Figure 7 and Figure 8 show the operation results of the novel integrated cooling and power system. As observed from the figure, the electric load demands are satisfied totally with the support of the WTs and external grid. Meanwhile, the LIM is utilized to carry out peak shaving and valley filling while producing ices. Suppose → denotes the driving direction, trucks transport these ices and dropped them into ISACs along 'LIM →ISAC 2→LIM→ISAC 1→LIM' in scenario 1, 'LIM→ISAC 1→LIM→ISAC 2→LIM' in scenario 2, and 'LIM→ISAC 2→LIM' in scenario 3. By this means, the working power of ISACs are reduced significantly, and the power flow can be better optimized. Note that although fewer WTs are installed in case 3 than those in case 2, the difference between the grid-connected wind power and network loss is larger, implying the power flow distribution in case 3 is better.

In case 3, the annual comprehensive operational cost of the distribution network is 36665200 yuan. Compared with that in case 1 and case 2, the operational cost can be saved by 160000800 yuan (81.4%), and 13126300 yuan (26.4%), respectively. The results show that the economy of the proposed expansion planning scheme is the best.

C. COOPERATION REVENUE DISTRIBUTION

Based on the simulation parameters in subsection A, section IV, the comprehensive costs of the seven economies engaged in the expansion planning of the distribution network are studied. The results are shown in Table 4. Note that as illustrated in section II, this article assumes that ISACs only participate

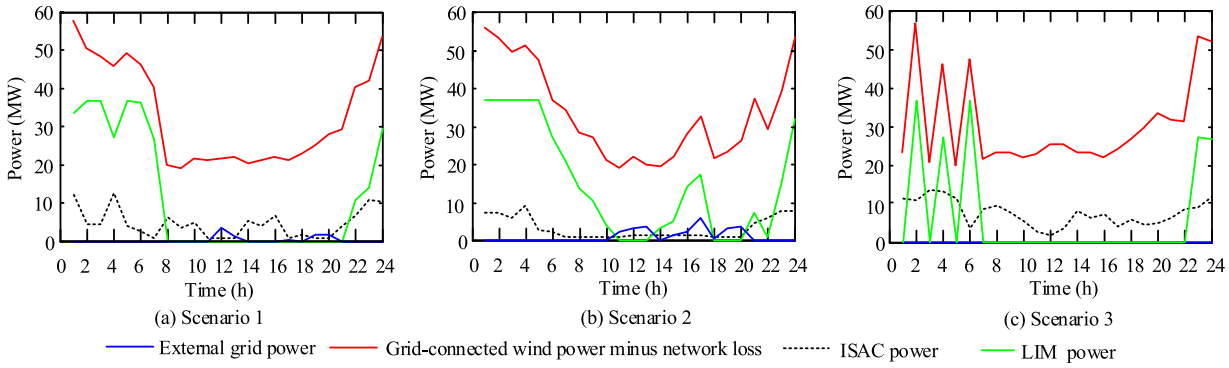

FIGURE 7. Operation power of integrated cooling and power system in case 3.

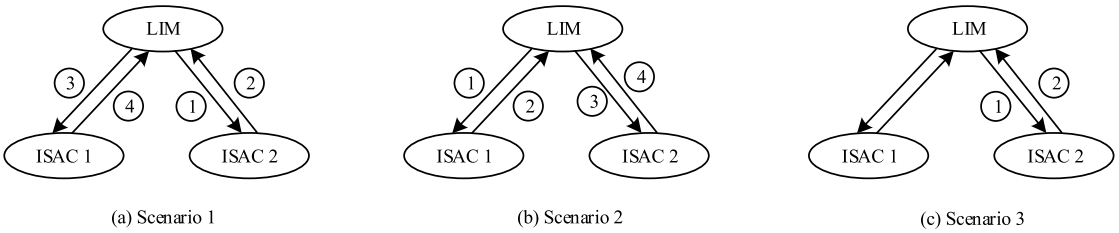

FIGURE 8. Trajectory of trucks with ices in case 3.

TABLE 4. Costs of economies engaged in the expansion planning.

Economies	Expansion planning cost
{GO, ISAC1, ISAC2}	36665200
{GO, ISAC1}	40627000
{GO, ISAC2}	43099000
{ISAC1, ISAC2}	0
{GO}	49791500
{ISAC1}	0
{ISAC2}	0

TABLE 5. Cost distribution based on the Shapley value method.

S	{GO}	{GO, ISAC1}	{GO, ISAC2}	{GO, ISAC1, ISAC2}
$V(S)$	49791500	40627000	43099000	36665200
$V(S\backslash\{GO\})$	0	0	0	0
$V(S)$-$V(S\backslash\{GO\})$	49791500	40627000	43099000	36665200
$\|S\|$	1	2	2	3
$W(\|S\|)$	1/3	1/6	1/6	1/3
$W(\|S\|)[V(S)$-$V(S\backslash\{GO\})]$	16597000	6771200	7183200	12222000

in the novel integrated cooling and power system scheduling, regardless of the unit configuration. Additionally, for simplicity, the electricity usage costs of the ISACs and common loads (i.e., the grid operator income, which can be traded separately) would not discussed in this article. Therefore, the expansion planning costs of {ISAC1, ISAC2}, {ISAC1}, and {ISAC2} are 0.

Taking the grid operator an example, Table 5 shows the cost distribution process based on the Shapley value method. It can be calculated that the actual cost of the grid operator is 16597000+6771200+7183200+12222000 = 42773400 yuan. Similarly, the actual costs of the ISAC1 owner and ISAC2 owner are −3672000 yuan, and −2436000 yuan, respectively. Compared with the non-cooperative mode, using the proposed expansion planning scheme, the grid operator, ISAC1 owner and ISAC2 owner can save 7018100 yuan, 3672000 yuan, and 2436000 yuan annually, respectively. The results show that all the participators would benefit from the proposed expansion planning model.

D. IMPACT OF THE TRUCK TRASIT TIME

Traffic factors such as congestion directly determine the actual transit time of the truck, which may affect the economy of the proposed scheme. The corresponding numerical simulation is carried out to study the impact.

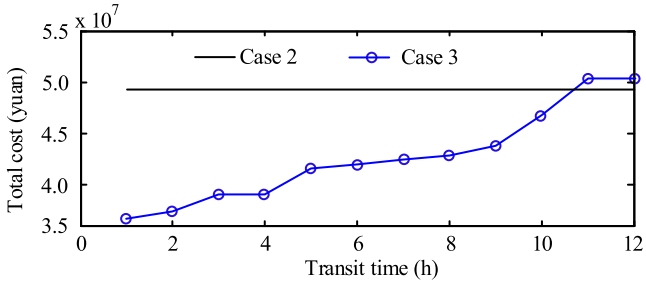

FIGURE 9. Impact of the truck transit time.

Figure 9 shows the comprehensive operation cost of the distribution network under different truck transit time. As observed from the figure, as the truck transit time increases from 1 hour to 11 hours, the operational costs of the distribution network in case 3 are increased. However, because the truck is required to return to initial position at the end of daily scheduling, the costs remains unchanged when transit time is larger than 11 hours. Additionally, when the transit time is less than 10 hours, the operation economy of

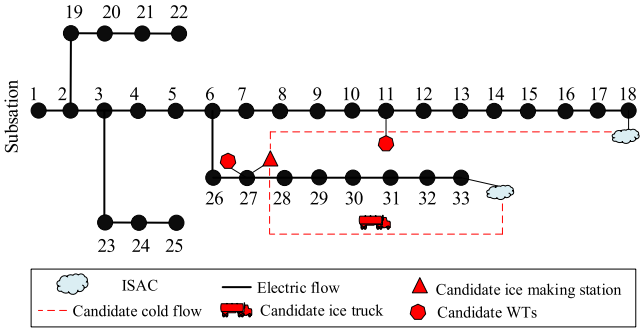

FIGURE 10. IEEE 33-node distribution network with the novel integrated cooling and power system.

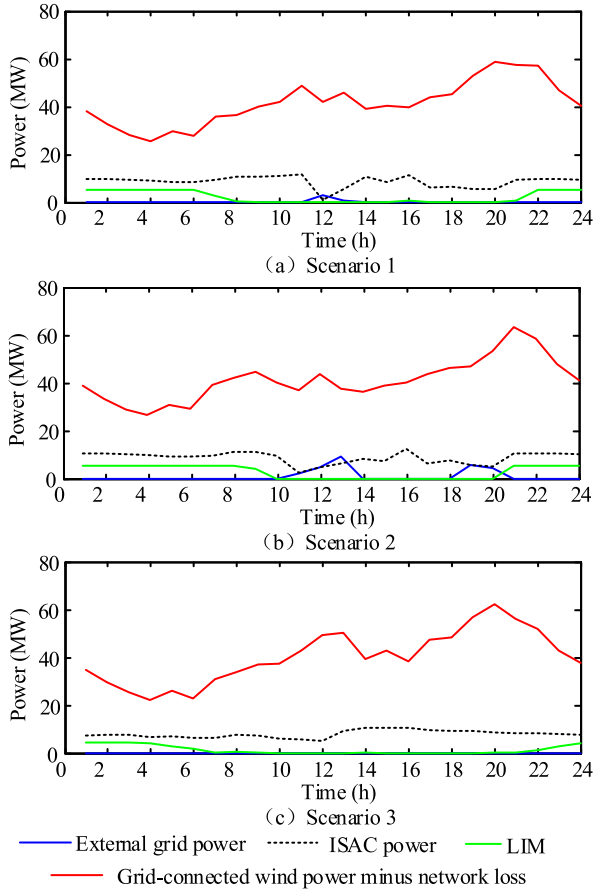

FIGURE 11. Operation power of integrated cooling and power system in case 3.

the distribution network in case 3 is always better than that in case 2. In additionally, the economy of the proposed scheme would be more obvious for a smaller transit time.

E. GENERAL APPLICABILITY OF THE EXPANSION PLANNING MODEL

To validate the general applicability, the proposed expansion planning model is conducted on an IEEE 33-node distribution network, as depicted in Fig. 10 [38]. The reference voltage and capacity are 12.66 kV, and 10 MVA, respectively. Compared with those in Figure A1, the electric loads and cooling

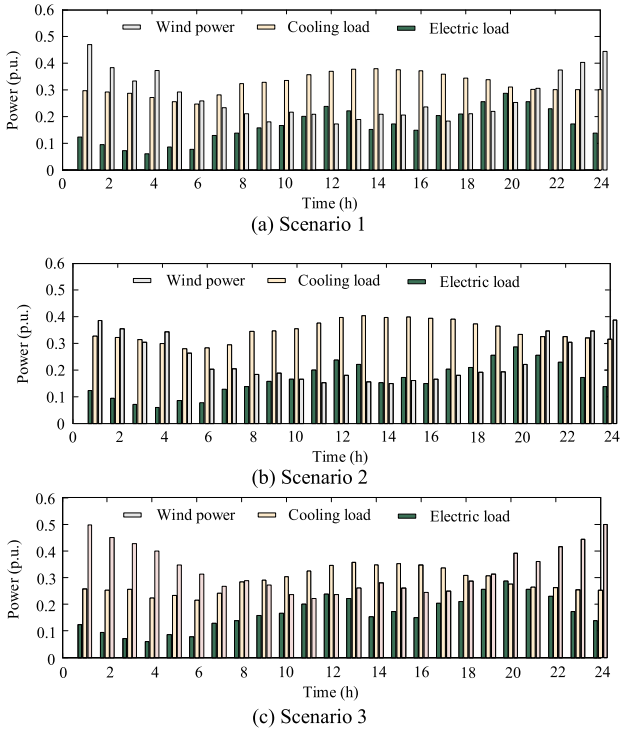

FIGURE 12. Profiles of the wind generation, electric load, and cooling load.

TABLE 6. Results of unit capacity configuration in three cases.

	WT at node 11(MW)	WT at node 27 (MW)	LIM at node 27(MW)
Case 1	0	0	0
Case 2	52	102	0
Case 3	36	106	5.6

loads are increased by 1.8494 and 1.2611 times, respectively. Two ISACs are connected to the distribution network at nodes 18 and 33. Candidate WTs are allowed to install at nodes 11 and 27, while candidate ice making station is required to locate at node 27. The wind power, EG power price, and cost parameters remain the same as in subsection A, Section V. The simulation results are presented as follows:

Table 6, Table 7, and Figure 11 show the expansion planning results of the distribution network using the proposed model. 142-MW WTs, and a 5.6-MW LIM are configured to produce electricity and ices, respectively. In three typical scenarios, the truck follows " 1→2→1", " 1→3→1→2→1", and " 1→3→1" to transport ices, respectively. By this means, the integrated cooling and power system can operate more flexibly.

Table 8 shows the comprehensive operational costs of the distribution network in three cases. As observed from the figure, 298207900 yuan, 48729200 yuan, and 45598060 yuan are spent in three cases, respectively. Compared with that in case 1 and case 2, the comprehensive cost of the distribution network in case 3 is reduced by 252609840 yuan (84.7%), 3131140 yuan (6.4%), respectively. The results prove the economic advantage of the proposed strategy again.

TABLE 7. Trajectory of trucks with ices in case 3.

Scenario 1	Time	11:00-12:00		20:00-21:00	
	Trip	1→2		2→1	
Scenario 2	Time	1:00-2:00	6:00-7:00	8:00-9:00	22:00-23:00
	Trip	1→3	3→1	1→2	2→1
Scenario 3	Time	5:00-6:00		12:00-13:00	
	Trip	1→3		3→1	

TABLE 8. Costs of distribution network in three cases.

	Annual depreciation cost (yuan)		Annual operation cost (yuan)			Total cost (yuan)
	WT	LIM	Load shedding	Purchasing electricity	Truck and driver	
Case 1	0	0	2497900	295710000	0	298207900
Case 2	45420000	0	0	3309200	0	48729200
Case 3	40842000	325460	0	3606600	824000	45598060

VI. CONCLUSION

In this article, a novel collaborative expansion planning model of integrated cooling and power system for low-latitude distribution networks is proposed. Not only the configuration of the wind turbine capacity, but also the optimization of the size of large ice makers and truck routes are considered in this model. On this basis, linearized techniques and the Benders decomposition algorithm are used to solve the optimization problem efficiently. The simulation results indicate that using the proposed strategy, the load shedding phenomenon can be avoided, and the operational cost of the low-latitude distribution network could be reduced significantly. Both the ISAC owners and grid operator would benefit from the novel integrated cooling and power system.

APPENDIX

See figure 12 here.

REFERENCES

[1] J. Liu, Y. Zhou, Y. Li, G. Lin, W. Zu, Y. Cao, X. Qiao, C. Sun, Y. Cao, and C. Rehtanz, "Modelling and analysis of radial distribution network with high penetration of renewable energy considering the time series characteristics," *IET Gener., Transmiss. Distrib.*, vol. 14, no. 14, pp. 2800–2809, Jul. 2020.

[2] H. Fan, Q. Yuan, S. Xia, J. Lu, and Z. Li, "Optimally coordinated expansion planning of coupled electricity, heat and natural gas infrastructure for multi-energy system," *IEEE Access*, vol. 8, pp. 91139–91149, 2020.

[3] A. P. Prato, F. Strobino, M. Broccardo, and L. P. Giusino, "Integrated management of cogeneration plants and district heating networks," *Appl. Energy*, vol. 97, pp. 590–600, Sep. 2012.

[4] T. Ma, J. Wu, L. Hao, W.-J. Lee, H. Yan, and D. Li, "The optimal structure planning and energy management strategies of smart multi energy systems," *Energy*, vol. 160, pp. 122–141, Oct. 2018.

[5] Y. Wang, N. Zhang, Z. Zhuo, C. Kang, and D. Kirschen, "Mixed-integer linear programming-based optimal configuration planning for energy hub: Starting from scratch," *Appl. Energy*, vol. 210, pp. 1141–1150, Jan. 2018.

[6] W. Huang, N. Zhang, J. Yang, Y. Wang, and C. Kang, "Optimal configuration planning of multi-energy systems considering distributed renewable energy," *IEEE Trans. Smart Grid*, vol. 10, no. 2, pp. 1452–1464, Mar. 2019.

[7] X. Dong, C. Quan, and T. Jiang, "Optimal planning of integrated energy systems based on coupled CCHP," *Energies*, vol. 11, pp. 1–27, Oct. 2018.

[8] A. Sheikhi, A. M. Ranjbar, and H. Oraee, "Financial analysis and optimal size and operation for a multicarrier energy system," *Energy Buildings*, vol. 48, pp. 71–78, May 2012.

[9] A. Franco and M. Versace, "Optimum sizing and operational strategy of CHP plant for district heating based on the use of composite indicators," *Energy*, vol. 124, pp. 258–271, Apr. 2017.

[10] A. Sheikhi, A. M. Ranjbar, and F. Safe, "A novel method to determine the best size of CHP for an energy hub system," in *Proc. 2nd Int. Conf. Elect. Power Energy Convers. Syst. (EPECS)*, Sharjah, UAE, 2011, pp. 1–7.

[11] S. Oh, H. Lee, J. Jung, and H. Kwak, "Optimal planning and economic evaluation of cogeneration system," *Energy*, vol. 32, no. 5, pp. 760–771, May 2007.

[12] G. Pan, W. Gu, Z. Wu, Y. Lu, and S. Lu, "Optimal design and operation of multi-energy system with load aggregator considering nodal energy prices," *Appl. Energy*, vol. 239, pp. 280–295, Apr. 2019.

[13] S. Pazouki, A. Mohsenzadeh, S. Ardalan, and M. Haghifam, "Optimal place, size, and operation of combined heat and power in multi carrier energy networks considering network reliability, power loss, and voltage profile," *IET Gener., Transmiss. Distrib.*, vol. 10, no. 7, pp. 1615–1621, May 2016.

[14] H. Cheng, J. Wu, Z. Luo, F. Zhou, X. Liu, and T. Lu, "Optimal planning of multi-energy system considering thermal storage capacity of heating network and heat load," *IEEE Access*, vol. 7, pp. 13364–13372, 2019.

[15] H. Ren, W. Gao, and Y. Ruan, "Optimal sizing for residential CHP system," *Appl. Thermal Eng.*, vol. 28, nos. 5–6, pp. 514–523, Apr. 2008.

[16] A. Franco and F. Bellina, "Methods for optimized design and management of CHP systems for district heating networks (DHN)," *Energy Convers. Manage.*, vol. 172, pp. 21–31, Sep. 2018.

[17] S. Lu, W. Gu, K. Meng, S. Yao, B. Liu, and Z. Y. Dong, "Thermal inertial aggregation model for integrated energy systems," *IEEE Trans. Power Syst.*, vol. 35, no. 3, pp. 2374–2387, May 2020.

[18] G. Pan, W. Gu, Y. Lu, H. Qiu, S. Lu, and S. Yao, "Optimal planning for electricity-hydrogen integrated energy system considering power to hydrogen and heat and seasonal storage," *IEEE Trans. Sustain. Energy*, vol. 11, no. 4, pp. 2662–2676, Oct. 2020.

[19] Y. Cao, W. Wei, J. Wang, S. Mei, M. Shafie-Khah, and J. P. S. Catalao, "Capacity planning of energy hub in multi-carrier energy networks: A data-driven robust stochastic programming approach," *IEEE Trans. Sustain. Energy*, vol. 11, no. 1, pp. 3–14, Jan. 2020.

[20] H. Zhou, Z. Li, J. H. Zheng, Q. H. Wu, and H. Zhang, "Robust scheduling of integrated electricity and heating system hedging heating network uncertainties," *IEEE Trans. Smart Grid*, vol. 11, no. 2, pp. 1543–1555, Mar. 2020.

[21] M. Song, C. Gao, H. Yan, and J. Yang, "Thermal battery modeling of inverter air conditioning for demand response," *IEEE Trans. Smart Grid*, vol. 9, no. 6, pp. 5522–5534, Nov. 2018.

[22] P. Ju, T. Jiang, H. Li, C. Wang, and J. Liu, "Hierarchical control of air-conditioning loads for flexible demand response in the short term," *IEEE Access*, vol. 7, pp. 184611–184621, 2019.

[23] R. Ramsden, T. J. Sheer, and M. D. Butterworth, "Design and simulation of ultra-deep mine cooling systems," in *Proc. 7th Int. Mine Ventilation Congr., Res. Develop. Center Electr. Eng. Automat. Mining (EMAG)*, Krakow, Poland, 2001, ch. 106, pp. 755–760.

[24] A. J. Schutte, M. Kleingeld, and H. J. Groenewald, "A holistic energy-cost evaluation of ice vs chilled water in mining," in *Proc. Int. Conf. Ind. Commercial Use Energy (ICUE)*, 2016, pp. 118–122.

[25] T. Persoons and J. A. Weibel, "Foreword: Special section on data center cooling," *IEEE Trans. Compon., Packag., Manuf. Technol.*, vol. 7, no. 8, pp. 1189–1190, Aug. 2017.

[26] J. Li, Z. Bao, and Z. Li, "Modeling demand response capability by Internet data centers processing batch computing jobs," *IEEE Trans. Smart Grid*, vol. 6, no. 2, pp. 737–747, Mar. 2015.

[27] F. Wei, Y. Li, Q. Sui, X. Lin, L. Chen, Z. Chen, and Z. Li, "A novel thermal energy storage system in smart building based on phase change material," *IEEE Trans. Smart Grid*, vol. 10, no. 3, pp. 2846–2857, May 2019.

[28] Z. Wang, S. Sun, X. Lin, C. Liu, N. Tong, Q. Sui, and Z. Li, "A remote integrated energy system based on cogeneration of a concentrating solar power plant and buildings with phase change materials," *Energy Convers. Manage.*, vol. 187, pp. 472–485, May 2019.

[29] J. Huang, T. Ha, and Y. Zhang, "An optimal control method of ice-storage air conditioning based on reducing direct cooling cost sequentially," in *Proc. IEEE Int. Conf. Power Renewable Energy (ICPRE)*, Shanghai, China, Oct. 2016, pp. 264–268.

[30] W.-S. Lee, Y.-T. Chen, and T.-H. Wu, "Optimization for ice-storage air-conditioning system using particle swarm algorithm," *Appl. Energy*, vol. 86, no. 9, pp. 1589–1595, Sep. 2009.

[31] *ICE Transport for Relieving Summer Heat*. Accessed: Jun. 30, 2016. [Online]. Available: http://news.eastday.com/s/20160630/u1ai9488831.html

[32] Y.-J. Zhang, A.-D. Wang, and Y.-B. Da, "Regional allocation of carbon emission quotas in China: Evidence from the shapley value method," *Energy Policy*, vol. 74, pp. 454–464, Nov. 2014.
[33] M. Hu, Y.-W. Wang, X. Lin, and Y. Shi, "A decentralized periodic energy trading framework for pelagic islanded microgrids," *IEEE Trans. Ind. Electron.*, vol. 67, no. 9, pp. 7595–7605, Sep. 2020.
[34] H. H. Abdeltawab and Y. A.-R.-I. Mohamed, "Mobile energy storage scheduling and operation in active distribution systems," *IEEE Trans. Ind. Electron.*, vol. 64, no. 9, pp. 6828–6840, Sep. 2017.
[35] *IEEE 14 Node Distribution Network*. Accessed: Jul. 26, 2011. [Online]. Available: https://wenku.baidu.com/view/a5eda49a51e79b896802269b?pcf=2&%20791%20bfetype=new
[36] *Electricity Price in China*. Accessed: Jul. 20, 2018. [Online]. Available: https://www.sohu.com/a/242323840_825986
[37] X. Cao, J. Wang, and B. Zeng, "A chance constrained information-gap decision model for multi-period microgrid planning," *IEEE Trans. Power Syst.*, vol. 33, no. 3, pp. 2684–2695, May 2018.
[38] *IEEE 33 Node Distribution Network*. Accessed: Nov. 16, 2017. [Online]. Available: https://wenku.baidu.com/view/41a874f548649b6648d7c1c708a1284ac8500502.html

BO YANG is currently an Engineer with Suzhou Power Supply Company of State Grid. His research interests include renewable energy technology and active distribution networks.

JUN TANG is currently with Suzhou Power Supply Company of State Grid, Suzhou, China. His research interests include active distribution networks and power system operation.

ZHAO LUO received the B.S. degree in electronic science and technology from the Nanjing University of Posts and Telecommunications, China, in 2008, and the M.S. and Ph.D. degrees in electrical engineering from Southeast University, China, in 2013 and 2018, respectively.

He is currently an Associate Professor with the Faculty of Electric Power Engineering, Kunming University of Science and Technology. His research interests include distributed generations and microgrids, and active distribution networks.

CHEN YANG is currently with Suzhou Power Supply Company of State Grid, Suzhou, China. His research interests include active distribution networks and power system operation.

XIAOFENG DONG is currently with Suzhou Power Supply Company of State Grid, Suzhou, China. His research interests include active distribution networks and power system operation.

JIALU GENG is currently pursuing the master's degree with the Faculty of Electric Power Engineering, Kunming University of Science and Technology, Kunming, China. His research interests include distributed generations and microgrids.

YUNRUI JIA is currently pursuing the master's degree with the Faculty of Electric Power Engineering, Kunming University of Science and Technology, Kunming, China. Her research interests include distributed generations and microgrids.

HONGZHI LIU is currently pursuing the master's degree with the Faculty of Electric Power Engineering, Kunming University of Science and Technology, Kunming, China. His research interests include distributed generations and microgrids.